

## Sonographic image texture features in muscle tissue-mimicking material reduce variability introduced by probe angle and gain settings compared to traditional echogenicity

Dustin J. Oranchuk,<sup>1,2\*</sup> Katie L. Boncella,<sup>1,3\*</sup> Daniela Gonzalez-Rivera,<sup>1,4</sup> Michael O. Harris-Love<sup>1,2,4,5</sup>

<sup>1</sup>Muscle Morphology, Mechanics, and Performance Laboratory, School of Medicine, University of Colorado Anschutz Medical Campus, Aurora, Colorado, United States; <sup>2</sup>Department of Physical Medicine and Rehabilitation, University of Colorado, Anschutz Medical Campus, Aurora, Colorado, United States; <sup>3</sup>Department of Bioengineering, University of Colorado Denver, Anschutz Medical Campus, Aurora, Colorado, United States; <sup>4</sup>University of Colorado Physical Therapy Program, School of Medicine, University of Colorado Anschutz Medical Campus, Aurora, Colorado, United States; <sup>5</sup>Eastern Colorado VA Geriatric Research, Education, and Clinical Center, Aurora, Colorado, United States.

*\*DJO and KLB contributed equally and have agreed to co-first authorship.*

*This article is distributed under the terms of the Creative Commons Attribution Noncommercial License (CC BY-NC 4.0) which permits any noncommercial use, distribution, and reproduction in any medium, provided the original author(s) and source are credited.*

### Abstract

Cost-effective and portable ultrasonography offers a promising approach for monitoring skeletal muscle damage and quality in many contexts. However, echogenicity analysis relies on precise transducer orientations and machine parameters, posing challenges for data pooling across different raters and settings. Muscle texture analysis offers a potential means of reducing inter-rater and machine-setting variability. Scans were assessed at nine angles, controlled using a custom transducer shell and software. Scans were performed three times, and different gains were applied. All scans were performed on a muscle tissue-mimicking phantom to eliminate biological variability. Intra-angle and intra-gain variability and internal consistency were assessed via coefficient of variation (CV%) and Cronbach's alpha ( $\alpha_c$ ). Spearman's ( $\rho$ ) correlations were employed to determine the relationship between echogenicity and each texture feature. Entropy (angle: CV=2.7-7.6%; gain: CV=10.5%;  $\alpha_c=0.86$ ), and inverse difference moment (angle: CV=3.7-9.8%; gain: CV=16.5%;  $\alpha_c=0.87$ ) were less variable than echogenicity (angle: CV=6.4-19.4%; gain: CV=39.0%;  $\alpha_c=0.82$ ). Angular second moment (angle: CV=17.9-116.6%; gain: CV=71.6%;  $\alpha_c=0.68$ ), contrast (angle: CV=7.8-14.7%; gain: CV=41.8%;  $\alpha_c=0.75$ ), and correlation (angle: CV=9.0-13.5%; gain: CV=28.6%;  $\alpha_c=0.49$ ) features were generally more variable. Entropy ( $\rho=0.82-0.98$ ,  $p\leq 0.011$ ) and inverse difference moment ( $\rho=-0.98-0.83$ ,  $p\leq 0.008$ ), were more strongly correlated with echogenicity than angular second moment ( $\rho=-0.98-0.77$ ,  $p\leq 0.016$ ), contrast ( $\rho=0.53-0.98$ ,  $p\leq 0.15$ ), and correlation ( $\rho=-0.25-0.19$ ,  $p=0.520-0.631$ ). Entropy and inverse difference moment features may allow data sharing between laboratory and clinical settings with ultrasound machine parameters and raters of varying skill levels. Clinical and mechanistic studies are required to determine if texture features can replace echogenicity assessments.

**Key Words:** phantom, echo intensity, gray level of co-occurrence matrix, muscle tissue mimetic, ultrasound.

The assessment of skeletal muscle mass is practiced in hospital, clinical, and sporting environments due to strong correlations with physical performance. As we age, conditions like sarcopenia and other muscle-wasting disorders become more prevalent, researchers and practitioners are increasingly incorporating methods to measure and monitor mass, quality, and composition. Echogenicity (grayscale analysis) is a prominent,<sup>1</sup> first-order,<sup>2</sup> technique for estimating muscle composition, where higher proportions of white pixels indicate increased muscle damage,<sup>3</sup> intramuscular adipose,<sup>4</sup> and fibrous<sup>5,6</sup> tissue compared to darker images (Figure 1). Indeed, recent meta-analyses revealed small to moderate yet highly consistent negative correlations between skeletal muscle echogenicity and physical function in older adults.<sup>7</sup>

Echogenicity and other assessments of muscle composition can be obtained using various technologies (e.g., MRI, CT),<sup>8</sup> though ultrasonography is gaining popularity due to its portability, relative affordability, and clinical utility. However, unlike MRI or CT, ultrasound imaging is more susceptible to human error as precise transducer orientation, tilt, and pressure are necessary to monitor longitudinal changes accurately.<sup>9</sup> Confounding factors like hydration, muscle glycogen shifts, and skin and subcutaneous fat tissue thickness can also affect echogenicity outputs and inter-session variability.<sup>1,3,4,6</sup> Additionally, scanning the same muscle using different ultrasound machines or inconsistent settings (e.g., gain and depth) can produce varying echogenicity values,<sup>10</sup> making comparing results between different clinics or laboratories challenging. Several research

groups have proposed clinically viable methods to improve variability to encourage data sharing and collaboration while potentially elucidating additional muscle-to-function relationships.<sup>11,12</sup> For example, while the muscle luminosity ratio may become clinically useful, it is significantly affected by ultrasonographic frequency parameters.<sup>13</sup> Similarly, Pinto & Pinto<sup>12</sup> have proposed specific analysis of echogenicity bands as an alternative to exclusively reporting mean values. However, the value and meaning of each grayscale band have not been thoroughly elucidated, and there are discordant reported findings when utilizing this analysis technique.<sup>14,15</sup> Computational approaches to analyzing the grayscale histogram have also been used to characterize muscle heterogeneity.<sup>16</sup> The dispersion parameters from a negative binomial distribution and shape parameters from gamma mixture models adequately fit grayscale histogram data and are associated with grip strength.<sup>16</sup> Nevertheless, additional work is needed to understand this approach's generalizability and clinical utility.

Muscle texture analysis is emerging as a promising approach for reliability assessing muscle quality.<sup>2</sup> This technique quantifies intricate patterns and variations within muscle images, going beyond conventional grayscale measurements to provide deeper insights concerning tissue heterogeneity and homogeneity.<sup>2</sup> The gray level co-occurrence matrix (GLCM) is a second-order statistical texture analysis approach that characterizes texture by examining the spatial relationship between pixel intensities across neighboring pixels and the entire image, rather than solely focusing on individual pixel intensities. Common GLCM features include Angular Second Moment (ASM), Entropy (ENT), Inverse Difference Moment (IDM), Correlation (COR), and Contrast (CON). These features estimate tissue homogeneity (ASM, IDM, COR) and heterogeneity (ENT, CON). Increased image heterogeneity, indicated by higher ENT and CON values, is associated with a greater presence of non-contractile muscle tissue. Additionally, a recent investigation<sup>17</sup> found significant correlations between several muscle texture features and physical performance in adults over 70. Importantly, texture analysis shows the potential to mitigate inter-rater and machine variability,<sup>18</sup> thereby enhancing the reliability and comparability of muscle assessments across different clinical settings and research laboratories. Therefore, this study aims to investigate and compare the variability in echogenicity and muscle texture features resulting from different transducer tilts and gain settings.

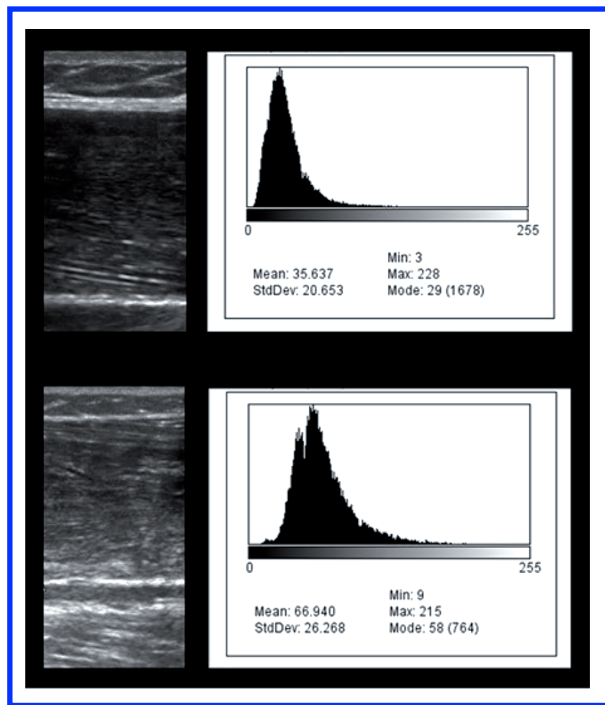


**Figure 1.** Representative images with grayscale analysis for high (top) and low (bottom) 'quality' human rectus femoris muscles.

## Materials and Methods

### Experimental design

A cross-sectional study used a custom-made ultrasound phantom (CIRS, Inc; Project #1126, Rev-02, Release-00, SN-E2164-2) comprised of muscle tissue mimicking material (TMM) to eliminate biological variability. A custom-built ultrasound transducer shell was employed to ensure precise angles. These measures were repeated three times. The 'Colorado Multiple Institutional Review Board approved the study (COMIRB: 24-0850).

**Testing procedures**

The custom-made muscle TMM phantom (length ~12 cm, diameter ~11 cm, thickness ~4.5 cm; anechoic gel: 15 kPa stiffness, 1540 m/s speed of sound, 0.1 dB/cm/MHz attenuation) was utilized to eliminate biological variability. The artificial muscle and representative scan are depicted in Figure 2. All scans were conducted using the same ultrasound machine (Hitachi Noblus) with 13.6 MHz linear array transducer (Hitachi, L64). All scans were performed with the same general settings (MSK application, dynamic range: 70, frame rate: 32, focus point: 2.6 mm, depth gain: maximum, Hi-Support: off) to a depth of 4 mm.

To ensure precise control over transducer tilts, we employed a custom-built transducer cover integrated with specialized software developed by Gilbertson and Anthony at Massachusetts Institute of Technology (Figure 3).<sup>19,20</sup> This setup utilizes fasteners and high-strength neodymium magnets to restrict movement along the Z-axis and secure the shell. Additionally, ridges prevent movement along the X and Y axes. The bottom shell houses a six-axis Mini-40 load-cell (FUTEK LSB200) and a three-axis analog-output accelerometer (Analog Devices ADXL 335). These components were connected to a signal amplifier (FUTEK IAA100), and DAQ (National Instruments USB-6001) interfaced with LabVIEW software and graphical user interface (GUI) to facilitate the collection and display of contact forces and transducer angles.<sup>19,20</sup>

Water-soluble transmission gel (Aquasonic 100; Parker Laboratories, Fairfield NJ) was used during scanning to attain optimal acoustic contact with the imaging site. Preliminary images were initially obtained in the transverse and longitudinal view to orient the examiners to the tissue-mimicking muscle phantom and to aid the calibration of the force-feedback transducer interface system. Longitudinal view image capture was completed at the midpoint of the ultrasound phantom with cine loops, allowing the operator to scroll through the captured frames. The images were taken at gain settings of 0, 5, and 10 dB, as most practitioners set their machines in 5 dB intervals. The measured transducer angles ranged from -50° to 50° (completely perpendicular=0°). An exemplar cine loop is provided in the *Supplementary materials, Video*.

**Image processing**

Using digitizing software (ImageJ; National Institutes of Health, USA), echogenicity and texture features were processed every 5° (21 total angles) at each gain setting. The largest possible region of interest was manually selected for all images. Mean echogenicity and the five texture features (Figure 4) of ASM, ENT, IDM, COR, and CON were analyzed at the GLCM angle of 180° and exported to a CSV file. Visual inspection of the cine loops determined extreme loss of muscle recognizability at angles >20° from perpendicular. Additionally, based on our experience in training novice assessors, we concluded that it would be unlikely that any assessor would obtain skeletal muscle images with a transducer angle error of >20°. Therefore, only the nine angles of -20°, -15°, -10°, -5°, 0°, 5°, 10°, 15° and 20° were analyzed. No image corrections were applied.

**Statistical analysis**

Intra-angle and intra-gain variability were assessed via the Coefficient of Variation (CV%). In contrast, Cronbach’s alpha ( $\alpha_c$ ), with 95% confidence intervals, was applied across angle and gain to provide an overall interpretation of internal consistency (*i.e.*, measuring the same underlying construct) for echogenicity and each texture feature. The CV% were interpreted as: high>30%, moderate=15-30%, and low<15%;<sup>21</sup> while  $\alpha_c$  were interpreted as: 0.50>un-acceptable, 0.50-0.60=poor, 0.61-0.70=questionable, 0.71-0.80=acceptable, 0.81-0.90=good, and excellent>0.90.<sup>22</sup> Each texture feature was compared to mean echogenicity via Spearman’s Rho ( $\rho$ ) rank correlation coefficient due to the small number of total images and uncertain linearity. Correlations were interpreted as:  $\pm 0-0.10$  trivial,  $\pm 0.10-0.30$  small,  $\pm 0.30-0.50$  moderate,  $\pm 0.50-0.70$  large,  $\pm 0.70-0.90$  very large, and  $\pm 0.90-1.00$  nearly perfect.<sup>23</sup> 95% confidence intervals were calculated for the correlational data by simulating 1000 bootstrapped samples. Jeffrey’s Amazing Statistics Package (JASP) software (v0.18.3, Amsterdam, Netherlands) was used for statistical analysis, while the correlation scatter plots were created in MATLAB (vR2021b, MathWorks, Natick, Massachusetts). 95% confidence intervals are provided in [square brackets].

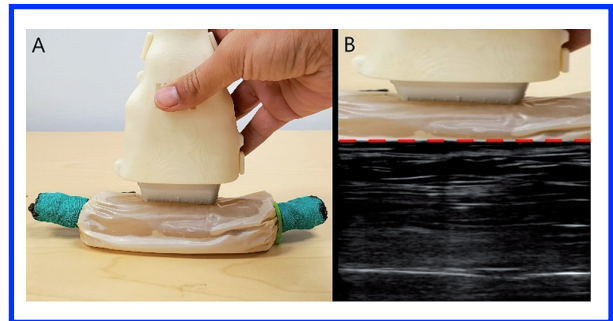


**Figure 2.** Tissue-mimicking muscle phantom (A) and representative image (B).

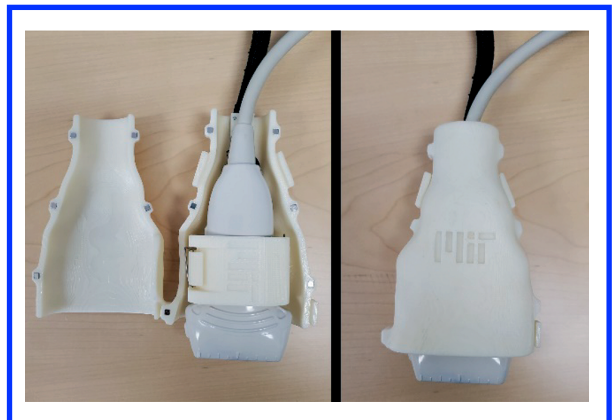


**Figure 3.** MIT developed transducer shell with a load-cell and accelerometer for ensuring precise angle and pressure.

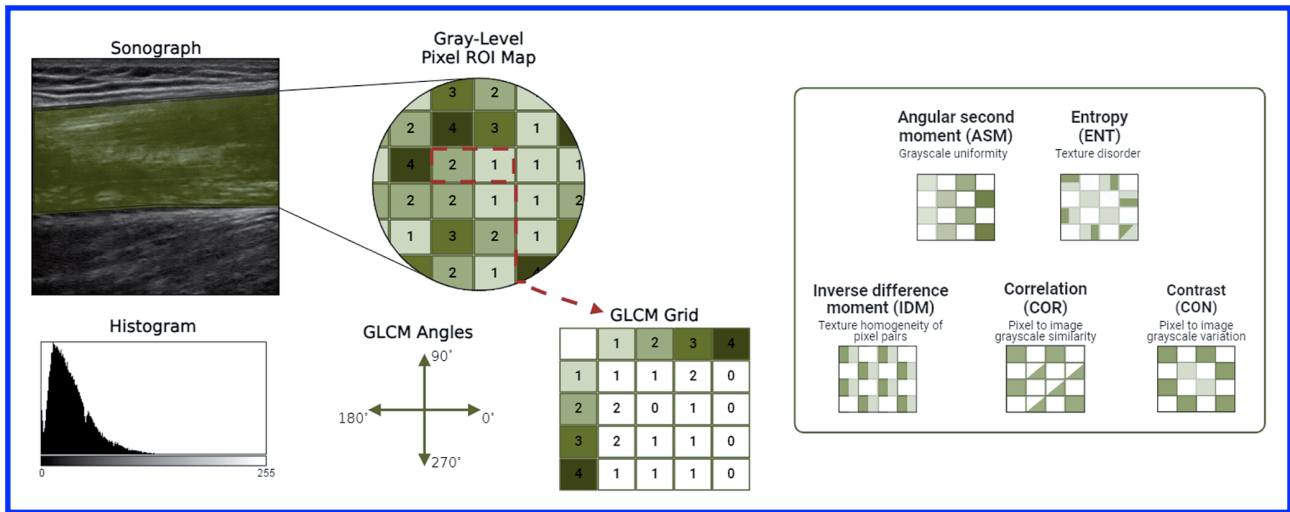


**Figure 4.** Gray level of co-occurrence matrix (GLCM) texture factors based on the distance of pixel and angle orientation of a B-mode ultrasound image. ROI=region of interest.

## Results

All echogenicity and muscle texture feature measures across all transducer angles and gain settings, with mean, standard deviation, CV% and  $\alpha_c$ , are provided in *Supplementary materials, Table 1*. Regarding variability, when examining across nine angles (CV=36.3%, range=26.2-38.9%) and three gains (CV=13.0%, range=6.4-19.4%), echogenicity held moderate to high, and low to moderate variability, respectively, with good internal consistency ( $\alpha_c=0.82$  [0.75-0.90]). ENT (angle: CV=10.3%, range=8.1-11.6%; gain: CV=5.0%, range=2.7-7.6%,  $\alpha_c=0.86$  [0.76-0.94]), and IDM (angle: CV=15.7%, range=9.7-19.1%; gain: CV=7.0%, range=3.7-9.8%,  $\alpha_c=0.87$  [0.71-0.96]) were generally less variable. Conversely, ASM (angle: CV=79.1%, range=49.5-107.5%; gain: CV=46.7%, range=17.9-116.6%,  $\alpha_c=0.68$  [0.45-0.85]), CON (angle: CV=40.2%, range=32.6-47.1%; gain: CV=11.8%, range=7.8-14.7%,  $\alpha_c=0.75$  [0.62-0.87]), and COR (angle: CV=22.1%, range=13.3-28.6%; gain: CV=7.7%, range=9.0-13.5%,  $\alpha_c=0.49$  [0.01-0.90]) were generally more variable than echogenicity, especially over different transducer tilt angles.

Regarding inter-feature correlations, when all angles and gains were pooled (27 data points), all texture features were significantly (all  $p<0.001$ ) and largely correlated with echogenicity (ASM:  $\rho=-0.97$  [-0.94 to -0.99]; CON:  $\rho=0.96$  [0.91-0.98]; COR:  $\rho=-0.80$  [0.60 to -0.90]; ENT:  $\rho=0.97$  [0.94-0.99]; IDM:  $\rho=-0.98$ , [-0.95 to -0.99]).

However, only ASM (0 dB:  $\rho=-0.77$  [-0.95 to -0.21],  $p=0.016$ ; 5 dB:  $\rho=-0.95$  [-0.99 to -0.76],  $p<0.001$ ; 10 dB:  $\rho=-0.98$  [-0.99 to -0.90],  $p<0.001$ ), ENT (0 dB:  $\rho=0.82$ , [0.33-0.96],  $p=0.011$ ; 5 dB:  $\rho=0.98$  [0.92-0.99],  $p<0.001$ ; 10 dB:  $\rho=0.83$ , [0.38-0.96],  $p=0.008$ ), and IDM (0 dB:  $\rho=-0.83$  [-0.96 to -0.38],  $p=0.008$ ; 5 dB:  $\rho=-0.98$  [-0.99 to -0.92],  $p<0.001$ ; 10 dB:  $\rho=-0.83$  [-0.96 to -0.38],  $p=0.008$ ) were significantly correlated with echogenicity across each

gain setting (9 data points) (Figure 5A, 5D, 5E). Conversely, CON (0 dB:  $\rho=0.90$  [0.59-0.98],  $p=0.002$ ; 5 dB:  $\rho=0.98$  [0.92-0.99],  $p<0.001$ ; 10 dB:  $\rho=0.53$  [-0.02 to 0.88],  $p=0.148$ ) was only significant correlated with echogenicity at with lower gain settings (Figure 5B), while COR (0 dB:  $\rho=-0.19$  [-0.76 to 0.55],  $p=0.631$ ; 5 dB:  $\rho=-0.25$  [-0.78 to 0.50],  $p=0.520$ ; 10 dB:  $\rho=-0.23$  [-0.78 to 0.51],  $p=0.550$ ) was not significantly correlated with echogenicity at any gain (Figure 5C).

## Discussion

While ultrasonic evaluations of muscle quality via grayscale analysis are common, they rely on precise transducer orientation and operator skill. Furthermore, different machine settings can substantially alter echogenicity, limiting data sharing between healthcare and laboratory settings. Thus, we compared variability introduced by transducer angle and ultrasound gain across echogenicity and several features of muscle texture. We determined that the muscle texture features of ENT and IDM were substantially less variable while holding strong correlations to echogenicity.

Contrary to echogenicity, there is a relative lack of studies examining the ability of muscle texture features to predict physical performance and other health measures.<sup>17,24,25</sup> However, Wilkinson *et al.*<sup>24</sup> examined the relationship between rectus femoris muscle texture features and grip strength, walking tasks, and sit-to-stand and timed up-and-go performances in participants with chronic kidney disease. Significant associations were reported between all muscle texture features and grip strength ( $\rho=\pm 0.24-0.29$ ,  $p\leq 0.026$ ), ASM, ENT and IDM and the incremental shuttle walk test ( $\rho=\pm 0.22-0.26$ ,  $p\leq 0.042$ ), and CON, COR, ENT, and IDM and gait speed ( $\rho=\pm 0.24-0.29$ ,  $p\leq 0.021$ ).<sup>24</sup> However, no features were significantly correlated with sit-to-stand or timed up-and-go performances ( $\rho=\pm 0.04-$

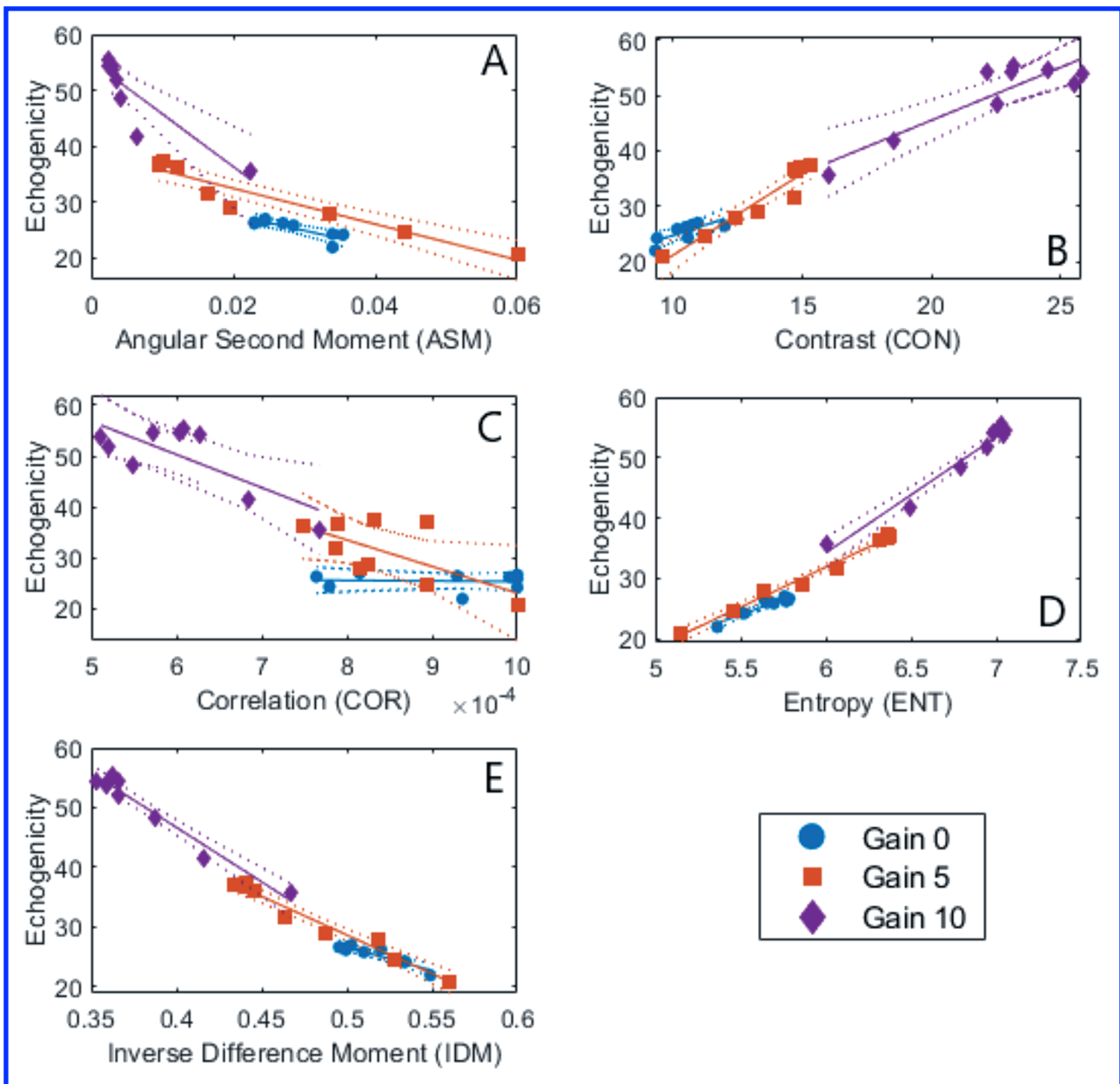


**Figure 5.** Correlation scatter plots with 95% confidence intervals between echogenicity and texture features of angular second moment (A), contrast (B), correlation (C), entropy (D), and inverse difference moment (E).

0.16,  $p \geq 0.126$ ).<sup>24</sup> While these correlations with performance are generally lower than much of the relevant echogenicity research,<sup>7</sup> ENT ( $r = -0.18$ ) and IDM ( $r = 0.17$ ) had the strongest mean correlation with the five functional assessments. Similarly, Fuentes-Abolafio *et al.*<sup>17</sup> examined the relationships between several texture features and sit-to-stand, timed up-and-go, short physical performance battery, and walking tests in people over 70 with degrees of heart failure. While there was some diversity of results across sexes and, ENT was generally the best predictor of physical performance ( $r = \pm 0.226-0.443$ ).<sup>17</sup> As a direct

comparison to the present study, Wilkinson *et al.* reported substantially smaller (though all significant;  $p < 0.001$ ) correlations between echogenicity and ASM ( $r = -0.53$ ), CON ( $r = 0.76$ ), COR ( $r = -0.52$ ), ENT ( $r = 0.76$ ), and IDM ( $r = -0.75$ ), perhaps highlighting the difference between human and our tissue-mimicking muscle phantom.<sup>24</sup> Echogenicity has also been extensively used to estimate muscle damage, correlating well with established proxies such as post-exercise force decrements, delayed onset muscle soreness, tissue swelling, and serum creatine kinase.<sup>3,26,27</sup> However, to our knowledge, only two studies

have examined relationships between muscle-damaging exercise and texture features.<sup>28,29</sup> de Matta and colleagues had participants perform twenty total isovelocity eccentric elbow flexions and assessed isometric torque, muscle soreness, muscle thickness, echogenicity, and CON and COR immediately before and 0, 24, 48, 72 and 96 hours post-exercise.<sup>28</sup> While echogenicity only increased at 72 and 96 hours, increases in COR first appeared at 48 hours and remained until at least 96 hours, implying greater sensitivity when estimating muscle damage.<sup>28</sup> Interestingly, no changes in CON were noted at any point,<sup>28</sup> suggesting that different texture features may have distinct utilities. This theory is supported by Jo and Kim, who also examined exercise-induced muscle damage of the biceps brachii.<sup>29</sup> Eccentric dumbbell curls induced substantial changes in echogenicity, ENT, ‘energy’, and IDM. However, the magnitude of these shifts differed between the short and long head of the biceps, with significantly greater alterations in ‘energy’ and IDM in the short head, while echogenicity and ENT increased more in the long head.<sup>29</sup>

### **Practical applications**

The improved variability of ENT and IDM compared to echogenicity across different transducer angles and gain settings offers promising avenues to advance muscle quality assessments in practical settings. Ultrasonography is relatively affordable and highly portable, making it suitable for widespread use in clinical settings such as hospitals, potentially saving valuable time and monetary resources. This shift from more expensive, large, and time-consuming imaging technologies (e.g., MRI and CT) is fundamental given the increasing elderly population in developed countries,<sup>30</sup> and soon globally.<sup>31</sup> However, the diversity of ultrasound machine models and manufacturers presents challenges when attempting to standardize data pooling and establish healthcare system-wide guidelines or cut-offs. While the interpretation of musculoskeletal muscle tissue scans across different devices may be aided through radio frequency time series signal analysis, clinical feasibility remains a barrier to adoption. Furthermore, if sonographic echogenicity replaced more resource-intensive technologies, many healthcare professionals would need to be upskilled in ultrasonography, potentially adding to their already heavy workload.<sup>32</sup> However, the current findings suggest that the muscle texture features of ENT and IDM could enable existing healthcare professionals to capture ultrasound images without strict adherence to precise transducer angles. It is also likely that texture analysis would not require subcutaneous fat correction,<sup>4</sup> further improving variability compared to echogenicity.<sup>6</sup> Additionally, a recent meta-analysis indicates that muscle quality may be systemic, allowing practitioners to scan easily accessible muscles (e.g., deltoid, biceps brachii) to obtain meaningful surrogate measures of muscle quality.<sup>7</sup> Assuming future advancements, these images could be uploaded to a database for automatic texture analysis and data pooling, facilitating widespread knowledge creation and advancing research in this field.

### **Limitations and future research directions**

Several limitations are to be noted. While we used a muscle tissue mimicking material phantom model to eliminate biological variation, a similar study should be performed in vivo. Likewise, the present study design did not allow us to determine the use of texture analysis for assessing longitudinal alterations in muscle quality due to disease or disuse or exercise, nutritional, or pharmacological interventions. While gain settings were considered a proxy for different ultrasound machines, similar work should be completed across several manufacturers and models. Although texture features were generally highly correlated with echogenicity, whether they are interchangeable is unclear. Therefore, mechanistic studies (e.g., biopsy, cadaver) are required to determine if echogenicity and the texture features similarly represent muscle composition. Similarly, acute to short-term exercise studies should examine the ability of muscle texture features to assess muscle damage.

### **Conclusions**

Muscle echogenicity is commonly used to estimate muscle composition and damage but is susceptible to variability based on ultrasound transducer angle and machine settings. The muscle texture features of ENT and IDM were less affected by transducer angle and gain than echogenicity and were highly correlated. Therefore, ENT and IDM may be superior to traditional echogenicity for assessing muscle quality, pooling data between assessors, and research or clinical settings. Human trials and longitudinal investigations are required to confirm this hypothesis.

### **List of abbreviations**

ASM, angular second moment  
CV, coefficient of variation  
CON, contrast  
COR, correlation  
 $\alpha_c$ , Cronbach’s alpha  
ENT, entropy  
GUI, graphical user interface  
GLCM, gray level co-occurrence matrix  
IDM, inverse difference moment  
 $\rho$ , Spearman’s Rho correlation  
TMM, tissue mimicking material

### **Data availability statement**

The data and ultrasonic images in this study are available to the corresponding author upon reasonable request.

### **Authors’ contributions**

MHL funded the study and the laboratory personnel (CTSI-CN UL1TR000075). MHL conceived the topic. DGR, KLB and MHL collected the data. KLB and DGR analyzed the images. MHL, KLB, and DJO performed the statistical analyses. DJO and KLB created the figures and tables. DJO wrote the initial version of the manuscript. All authors ed-

ited and approved the submitted manuscript. DJO and KLB contributed equally and have agreed to co-first authorship.

## Conflict of interest

The authors declare no conflict of interest.

## Funding disclosure

None.

## Corresponding author

Michael O. Harris-Love, Muscle Morphology, Mechanics, and Performance Laboratory, School of Medicine, University of Colorado Anschutz Medical Campus, Aurora, Colorado, USA.

ORCID ID: 0000-0002-1842-3269

E-mail: Michael.Harris-Love@CUAnschutz.edu

## Co-authors

*Dustin J Oranchuk*

ORCID ID: 0000-0003-4489-9022

E-mail: dustin.oranchuk@cuanschutz.edu

*Katie M Boncella*

ORCID ID: 0000-0003-0576-1610

E-mail: katie.boncella@cuanschutz.edu

*Daniela Gonzalez-Rivera*

ORCID ID: 0000-0001-7243-0681

E-mail: daniela.gonzalez-rivera@cuanschutz.edu

## References

1. Stock MS, Thompson BJ. Echo intensity as an indicator of skeletal muscle quality: applications, methodology, and future directions. *Eur J Appl Physiol* 2021;121:369-80.
2. Paris M, Mourtzakis M. Muscle composition analysis of ultrasound images: A narrative review of texture analysis. *Ultrasound Med Biol* 2021;47:880-95.
3. Wong V, Spitz RW, Bell ZW, et al. Exercise induced changes in echo intensity within the muscle: A brief review. *J Ultrasound* 2020;23:457-72.
4. Young H, Jenkins NT, Zhao Q, McCully KK. Measurement of intramuscular fat by muscle echo intensity. *Muscle Nerve* 2015;52:963-71.
5. Pillen S, Tak RO, Zwarts MJ, et al. Skeletal muscle ultrasound: Correlation between fibrous tissue and echo intensity. *Ultrasound Med Biol* 2009;35:443-6.
6. Oranchuk DJ, Stock MS, Nelson AR, et al. Variability of regional quadriceps echo intensity in active young men with and without subcutaneous fat correction. *Appl Physiol Nutr Metab* 2020;45:745-52.
7. Oranchuk DJ, Bodkin SG, Boncella KL, Harris-Love MO. Exploring the associations between skeletal muscle echogenicity and physical function in aging adults: A systematic review with meta-analyses. *J Sport Health Sci* 2024;13:820-40.
8. Zhang YN, Fowler KJ, Hamilton G, et al. Liver fat imaging—A clinical overview of ultrasound, CT, and MR imaging. *Br J Radiol* 2018;91:20170959.
9. Dankel SJ, Abe T, Bell ZW, et al. The impact of ultrasound probe tilt on muscle thickness and echo-intensity: A cross-sectional study. *J Clin Densitom* 2020;23:630-8.
10. Varanoske AN, Coker NA, Johnson BAD, Belity T, Wells AJ. Influence of muscle depth and thickness on ultrasound echo intensity of the vastus lateralis. *Acta Radiol.* 2021;62:1178-87.
11. Wu JS, Darras BT, Rutkove SB. Assessing spinal muscular atrophy with quantitative ultrasound. *Neurology* 2010;75:526-31.
12. Pinto RS, Pinto MD. Moving forward with the echo intensity mean analysis: Exploring echo intensity bands in different age groups. *Exp Gerontol* 2021;145:111179.
13. Hobson-Webb LD, Mhoon JT, Juel VC. Effect of transducer frequency on muscle luminosity ratio. *Muscle Nerve* 2011;44:612-3.
14. Logeson ZS, MacLennan RJ, Abad GKB, et al. The impact of skeletal muscle disuse on distinct echo intensity bands: A retrospective analysis. *PLoS ONE* 2022;17:e0262553.
15. Southhall, K, Wohlgemuth KJ, Hare MM, Mota JA. Does the analysis of separate bands of echo intensity strengthen the relationship to muscle function? *Int J Exerc Sci* 2023;2:50.
16. Harris-Love MO, Gonzales TI, Wei Q, et al. Association between muscle strength and modeling estimates of muscle tissue heterogeneity in young and old Adults. *J Ultrasound Medicine* 2019;38:1757-68.
17. Fuentes-Abolafio IJ, Ricci M, Bernal-López MR, et al. Relationship between quadriceps femoris echotexture biomarkers and muscle strength and physical function in older adults with heart failure with preserved ejection fraction. *Exp Gerontol* 2024;190:112412.
18. Martínez-Payá JJ, Ríos-Díaz J, Del Baño-Aledo ME, et al. Quantitative muscle ultrasonography using textural analysis in amyotrophic lateral sclerosis. *Ultrason Imaging* 2017;39:357-68.
19. Gilbertson MW, Anthony BW. An ergonomic, instrumented ultrasound probe for 6-axis force/torque measurement. In: Annual International Conference of the IEEE Engineering in Medicine and Biology Society. IEEE; 2013:140-3.
20. Huang AY. May the force be with you: a medical ultrasound system with integrated force measurement. Master of Science in Mechanical Engineering. Massachusetts Institute of Technology. Available from: <http://hdl.handle.net/1721.1/113755>
21. Devore JL. Probability and Statistics for Engineering and the Sciences. Ninth edition. Cengage Learning; 2016.
22. Streiner DL. Starting at the beginning: An introduction to coefficient alpha and internal consistency. *J Pers Asses* 2003;80:99-103.
23. Hopkins WG, Marshall SW, Batterham AM, Hanin J.

## Sonographic image texture features vs. traditional echogenicity in muscle tissue-mimicking material

Eur J Transl Myol 35 (2) 13511, 2025 doi: 10.4081/ejtm.2025.13511

- Progressive Statistics for Studies in Sports Medicine and Exercise Science. *Med Sci Sports Exerc* 2009; 41:3-12.
24. Wilkinson TJ, Ashman J, Baker LA, et al. Quantitative muscle ultrasonography using 2D textural analysis: A novel approach to assess skeletal muscle structure and quality in chronic kidney disease. *Ultrason Imaging* 2021;43:139-48.
  25. Watanabe T, Murakami H, Fukuoka D, et al. Quantitative sonographic assessment of the quadriceps femoris muscle in healthy Japanese adults. *J Ultrasound Med* 2017;36:1383-95.
  26. Oranchuk DJ, Nelson AR, Storey AG, et al. Short-term neuromuscular, morphological, and architectural responses to eccentric quasi-isometric muscle actions. *Eur J Appl Physiol* 2021;121:141-58.
  27. Radaelli R, Bottaro M, Wilhelm EN, et al. Time course of strength and echo intensity recovery after resistance exercise in women. *J Strength Cond Res* 2012;26: 2577-84.
  28. Matta TTD, Pereira WCDA, Radaelli R, et al. Texture analysis of ultrasound images is a sensitive method to follow-up muscle damage induced by eccentric exercise. *Clin Physio Funct Imaging* 2018;38:477-82.
  29. Jo HD, Kim MK. Identification of EIMD level differences between long- and short head of biceps brachii using echo intensity and GLCM texture features. *Res Q Exerc Sport* 2024;95:441-9.
  30. Mason CN, Miller T. International projections of age specific healthcare consumption: 2015–2060. *J Econ Ageing* 2018;12:202-17.
  31. Akinrolie O, Iwuagwu AO, Kalu ME, et al. Longitudinal studies of aging in sub-saharan Africa: Review, limitations, and recommendations in preparation of projected aging population. Chukwuorji J, ed. *Innov Aging* 2024;8:igae002.
  32. Maghsoud F, Rezaei M, Asgarian FS, Rassouli M. Workload and quality of nursing care: The mediating role of implicit rationing of nursing care, job satisfaction and emotional exhaustion by using structural equations modeling approach. *BMC Nurs* 2022;21:273.

### Disclaimer

All claims expressed in this article are solely those of the authors and do not necessarily represent those of their affiliated organizations, or those of the publisher, the editors and the reviewers. Any product that may be evaluated in this article or claim that may be made by its manufacturer is not guaranteed or endorsed by the publisher.

Submitted: 20 December 2024.

Accepted: 9 February 2025.

Early access: 1 April 2025.

---

*Online supplementary material:*

*Video.*

*Table 1. Summary of all echogenicity and muscle texture features across nine angles and three gain settings.*